Transmission line model for strained quantum well lasers including carrier transport and carrier heating effects

Xia, Mingjun; Ghafouri-Shiraz, Hooshang

DOI:
10.1364/AO.55.001518

A Novel Transmission Line Model for Strained Quantum Well Lasers Including Carrier Transport and Carrier Heating Effects

MINGJUN XIA, H. GHAFOURI-SHIRAZ *

School of Electronic, Electrical and System Engineering, University of Birmingham, Birmingham, B15 2TT, United Kingdom

Email xiamingjunsdu@hotmail.com

**Corresponding author: ghafourh@bham.ac.uk*

Received 19 Nov. 2015

The paper reports a new model for strained quantum well lasers which is based on quantum well transmission line modelling method where effects of both carrier transport and carrier heating have been included. We have applied this new model and studied the effect of carrier transport on the output waveform of a strained quantum well laser both in time and frequency domains. It has been found that the carrier transport increases the turn-on, turn-off delay times and damping of the quantum well laser transient response. Also, analysis in frequency domain indicates that the carrier transport causes the output spectrum of quantum well laser in steady state exhibits a red shift which has a narrower bandwidth and lower magnitude. The simulation results of turning-on transients obtained by the proposed model are compared with that obtained by the rate equation laser model. The new model has also been used to study the effects of pump current spike on the laser output waveforms properties and it was found that the presence of current spike causes (i) wavelength red shift, (ii) larger bandwidth, (iii) reduces the magnitude and decreases the side-lobes suppression ratio (SLSR) of the laser output spectrum. Analysis in both frequency and time domains confirms that the new proposed model can accurately predict the temporal and spectral behaviors of strained quantum well lasers.

OCIS codes: *250.5960 (Semiconductor lasers), 250.5590 (Quantum-well, -wire and -dot devices), 140.3430 (Laser theory)*

1. INTRODUCTION

Quantum well (QW) lasers are attractive in the optical fiber communication and sensing system due to their advantages, such as small size, high efficiency and cost-effectiveness [1-3]. The quantization of the density states and the energy band structure lead to improved properties of quantum well lasers as compared with bulk material lasers. Many QW lasers models have been developed and reported in the last two decade and so, among them: photon rate equations [4-5] and transmission line laser model [6-8] which have been used to study the properties of QW lasers in both time domain and frequency domains. However, the method of studying the spectral properties of QW laser by solving a set of rate equations [5] cannot provide the continuous spectrum and needs a lot of simulation time. The reported transmission line laser models [9-10] were established for the bulk lasers and adopted the frequency-independent gain or the symmetric frequency-dependent gain curve by using only one stub filter, which clearly indicates that such models without considering the dynamic photon-electron interaction can't accurately predict the spectral behavior of QW lasers.

Quantum well transmission line modelling (QW-TLM) is a new technique to establish models for semiconductor optical devices [11]. The method adopts parallel QW-TLM units to model the electron transition processes between the conduction and valence bands in the wave vector space. In each QW-TLM unit, two parallel RLC stub filters and their corresponding weight coefficients are adopted to describe the electron transition from the conduction band to the heavy and

light holes bands at a given wave vector. The open-circuited and short-circuited transmission lines are used to model the

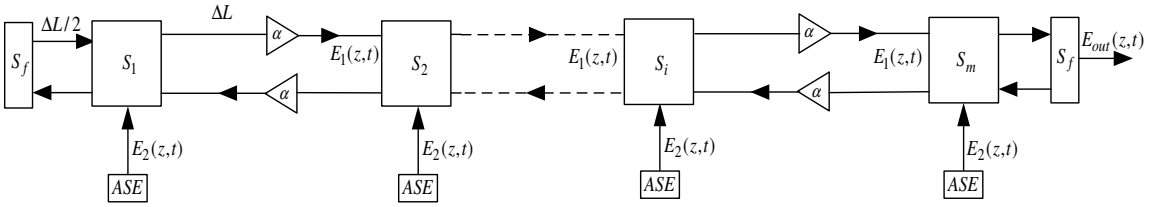

Fig. 1 The proposed QW laser model

capacitors and inductors in the stub filter of each QW-TLM unit [12]. The model established by the QW-TLM method has considered the electron-photon dynamic interaction and the coupling among the heavy and light holes bands as well as the spin-spilt off band induced by the strain effects. It has been confirmed that this method can accurately model the optical gain of quantum well devices [11].

Carrier transport plays an important role in determining the temporal and spectral responses of QW lasers [13-15]. Inferior modulation responses have been reported in the QW lasers due to carrier transport effects [16-17]. The carrier transport which includes, the separate confinement heterostructure and the inter-well transports, reduces the effective differential gain and increases the carrier recombination lifetime in the QW lasers. However, the effect of carrier transport on the output performance of the QW laser has not been studied considering the dynamic photon-electron interaction. Besides, the presence of pump current spike which is due to the electromagnetic field interference affects the laser output performance which needs to be analyzed. In this paper, we propose a new model for QW lasers using the QW-TLM method which takes into account effects of both carrier transport and carrier heating. The new model is adopted to analyze effects of carrier transport and pump current spike on the output properties of QW lasers.

The paper is organized as follows: Section 2 introduces a new theoretical model for QW lasers. In section 3 based on this model, carrier transport and pump current spike effects on the output performances of QW lasers are studied. Finally, conclusion is given in Section 4.

2. THEORY

A. Theoretical model description

The QW-TLM method is employed to establish the QW laser model, which can be used to study the temporal and spectral properties of QW lasers. Fig. 1 shows the proposed model for the QW laser which is based on QW-TLM [11]. In this model, the laser cavity is divided into m sections, each of which consists of scattering module, spontaneous emission module, transmission line and transmission efficient α. The facet model S_f is used to describe the facet reflection. Both the scattering and spontaneous emission modules are employed to model the photon stimulated and spontaneous emissions processes in the laser cavity. The electric fields propagate along the transmission line and stimulate the photon emission in the scattering module. Both the scattering module and the spontaneous emission module consist of parallel QW-TLM units. The length of the transmission line between two adjacent scattering modules is ΔL while the length of the transmission line linking the facet model and the closest scattering module is $\Delta L/2$. Fig. 2 shows the structure of the scattering module S in the laser model.

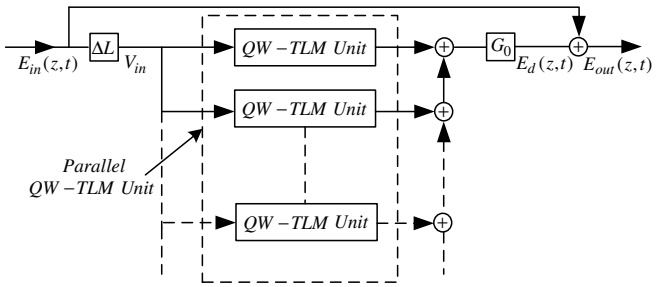

Fig. 2 Structure of the scattering module in the laser model

The length ΔL is so small that the electric field distribution along the small distance can be considered as a constant. Thus, the input signal voltage V_{in} can be expressed as:

$$V_{in} = E_{in}^{\pm}(z,t)\Delta L \qquad (1)$$

where $E_{in}^{\pm}(z,t)$ represents the electric field (forward and backward). The voltage signal propagates in each parallel QW-TLM unit and scatters at the unit stub filter. Each QW-TLM unit has two parallel RLC stub filters and their corresponding weight coefficients which are used to model the electron transitions from the conduction band to the heavy hole band and the light hole band at a given wave vector. The characteristic admittance expressions for the resistors, capacitors and inductors in the QW-TLM unit can be found in Ref [12]. The electric field propagation time ΔT in each section of the laser cavity is determined by the sampling frequency through the equation $\Delta T = 1/f_{sam}$. The Q-factor of the stub filter is determined by the bandwidth of electron scattering spectrum and the central frequency is determined by the energy difference between the conduction band and the heavy hole band or the light hole band at the corresponding wave vector. The energy band structure is obtained by solving the Schrodinger equations using the finite difference method [18-

21]. The output electric field of the scattering module can be expressed as:

$$E_{out}(z,t) = E_{in}(z,t) + E_d(z,t) \quad \textbf{(2)}$$

where, $E_d(z,t)$ is obtained by adding all outputs of parallel Q-TLM units multiplied by the gain coefficient G_0 given below [22]:

$$G_0 = \frac{\Gamma q^2}{\pi h n_r c \varepsilon_0 m_0^2 L_z \gamma} \quad \textbf{(3)}$$

where, Γ is the optical confinement factor, q is the magnitude of the electron charge, h is the Plank constant, n_r and ε_0 are the refractive index and the permittivity in free space, c is the speed of light in free space, m_0 is the electron rest mass in free space, L_z is the quantum well width and γ is the linewidth of electron scattering.

Figure 3 shows the structure of the spontaneous emission module in the laser model which consists of a ASE source, parallel QW-TLM units and the coupling coefficient β.

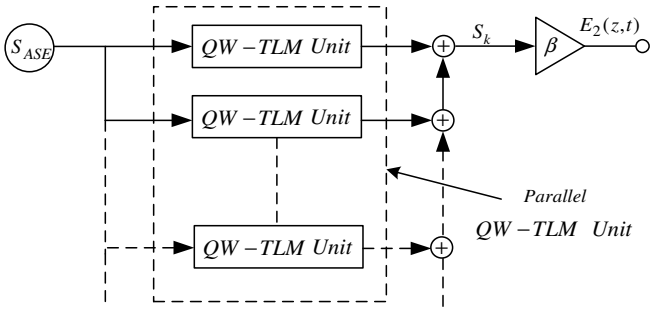

Fig. 3 Structure of the spontaneous emission module

The output of the ASE source S_{ASE} can be expressed as [21]

$$S_{ASE}(t) = \begin{cases} E_0/q & for \quad t = nT_1, n = 0,1,2... \\ 0 & for \quad (n-1)T_1 < t < nT_1, n = 1,2... \end{cases} \quad \textbf{(4)}$$

where, E_0 is the energy of a photon, T_1 is the lifetime of the exited state. The characteristic admittance values and the weight coefficients of the parallel QW-TLM units in the spontaneous emission source are given in Ref [22]. The output electric filed $E_2(z,t)$ can be expressed as

$$E_2(z,t) = \beta S_k \quad \textbf{(5)}$$

where, S_k is the sum of the outputs of the parallel QW-TLM units. Fig. 4 shows the electric fields flow at the end facets of the QW laser model.

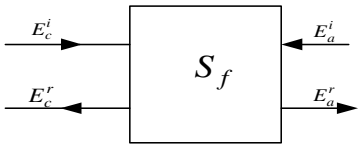

Fig. 4 Electric field flow for a laser facet model

In the facet model, the Fresnel reflection and transmission at the facet can be expressed as [23]:

$$\begin{bmatrix} E_c^r \\ E_a^r \end{bmatrix} = \begin{bmatrix} \rho_{cc} & \rho_{ac} \\ \rho_{ca} & \rho_{aa} \end{bmatrix} \begin{bmatrix} E_c^i \\ E_a^i \end{bmatrix} \quad \textbf{(6)}$$

where, E_c^i and E_a^i are the input electric fields of the facet from the adjacent scattering module and the air, E_c^r and E_a^r are the reflected electric fields, ρ_{cc} is the electric field reflection coefficient (EFRC) from the cavity to cavity, ρ_{aa} is the EFRC from air to air, ρ_{ca} is the electric field transmission coefficient (EFTC) from cavity to air, ρ_{ac} is the EFTC coefficient from air to cavity.

B. Carrier transport effects in the QW-TLM laser model

Under the assumption that the current is injected from the left side of the separate confinement heterostructure (SCH) laser, the rate of change of carrier density N_1 at the left SCH of the laser can be expressed as [24]

$$\frac{dN_1}{dt} = \frac{\eta I}{qV_1} - \frac{N_1}{\tau_s} - \frac{N_1}{\tau_n(N_1)} + \frac{V_{well}}{V_1}\frac{N_{well}}{\tau_e} + \xi\frac{N_2}{\tau_s} \quad \textbf{(7)}$$

The rate of change in the carrier density N_2 of the laser right SCH region is [23]

$$\frac{dN_2}{dt} = -\frac{N_2}{\tau_s} - \frac{N_2}{\tau_n(N_2)} + \frac{V_{well}}{V_2}\frac{N_{well}}{\tau_e} + \xi\frac{N_1}{\tau_s} \quad \textbf{(8)}$$

In the well region, the carrier rate equation including the transport effects can be written as:

$$\frac{dN_{well}}{dt} = (1-\xi)\frac{V_1}{V_{well}}\frac{N_1}{\tau_s} + (1-\xi)\frac{V_2}{V_{well}}\frac{N_2}{\tau_s} - \frac{N_{well}}{\tau_n(N_{well})} - \frac{2N_{well}}{\tau_e} - \frac{\Gamma}{qDW\Delta L}\frac{V_{in}}{Z_p} \quad \textbf{(9)}$$

where, I is the injected current, η is the internal quantum efficiency, V_1 and V_2 are the volumes of the left and right side of the SCH layers, τ_s is the carrier transport time in the SCH region, τ_e is the carrier thermionic emission time, ξ is the leak factor, V_{well} is the volume of the well, V_{in} is the input voltage of each scattering module, D and W are the thickness

and width of the well, N_{well} is the carrier density in the well region and ΔL is the length of the transmission line between two adjacent scattering modules. Both $\tau_n(N_1)$ and $\tau_n(N_{well})$ which are carrier recombination lifetimes in the SCH and in the quantum well regions, respectively, can be obtained by using the well- known formula $1/(A+BN+CN^2)$ [8], where, A, B and C are linear recombination constant, Bi-molecular recombination constant and Auger recombination constant, respectively.

C. Carrier heating effects in QW-TLM laser model

In quantum well lasers, the change in carrier temperature,T, which is due to the carrier heating in the well region can be described by the following temperature dynamic expression [25]

$$\frac{dT}{dt}=\frac{1}{\partial U/\partial T}\left(\frac{dU}{dt}-\frac{\partial U}{\partial N}\frac{dN_{well}}{dt}\right)-\frac{T-T_0}{\tau} \quad (10)$$

where, U is the total carrier energy density, τ is a phenomenological time constant to represent the temperature relaxation and T_0 is the lattice temperature. The total carrier energy density is the sum of the carrier energy densities of the conduction (U_C) and valance (U_V) bands, that is [26]:

$$U=U_C+U_V \quad (11)$$

where

$$U_C=\sum_n\frac{1}{\pi L_z}\int_0^{+\infty}\frac{E_n^c(k_t)-E_c}{1+\exp((E_n^c(k_t)-E_{fc})/K_BT)}k_t dk_t \quad (12)$$

$$U_V=\sum_m\sum_{HH,LH,SO}\frac{1}{\pi L_z}\int_0^{+\infty}\frac{E_v-E_m^v(k_t)}{1+\exp((E_{fv}-E_m^v(k_t))/K_BT)}k_t dk_t \quad (13)$$

In the above equations, E_c and E_v are the band edges of the conduction and valence bands $E_n^c(k_t)$ is the nth sub-band energy in the conduction band and $E_m^v(k_t)$ is the mth sub-band energy in the valance band, E_{fc} and E_{fv} are the quasi-Fermi levels in the conduction and valence bands, K_B is the Boltzmann constant. The partial derivatives $\partial U/\partial T$ and $\partial U/\partial N$ in Eq.(10) can be calculated through Eqs. (11) to (13). $\partial U/dt$ in Eq. (10) can be calculated by considering the rate of energy changes due to the simulated emission, spontaneous emission and free carrier absorption, that is:

$$\frac{dU}{dt}=-\frac{\varepsilon|E_d(z,t)|^2}{2\Delta V\Delta T}+\frac{\alpha_f\varepsilon|E_{in}(z,t)|^2}{2\Delta V\Delta T} \quad (14)$$

where, ε is the permittivity of the quantum well, α_f is the free carrier absorption coefficient, ΔV is the volume of each section of the QW laser and ΔT is the optical signal propagation time in each section.

3. RESULTS AND DISCUSSIONS

In this section, the effects of carrier transport and pump current spike on the output properties of the strained $In_{0.64}Ga_{0.36}As-InGaAsP$ QW laser are studied using the above theoretical model. The well and barrier widths are $4.5nm$ and $10nm$, respectively, and the other parameters used in the simulations are provided in the following Tab. 1and Ref. [21].

Table 1 Simulation parameters [26]

Symbol	Description	Value
n	Background refractive index	3.67
m	Number of sections	10000
Q	Stub filter Q-factor	60.8
f_{sam}	Sampling frequency	$1.0\times10^{15}Hz$
A	Linear recombination	$2\times10^{8}s^{-1}$
B	Bi-molecular recombination	$6\times10^{-16}m^3s^{-1}$
C	Auger recombination	$8\times10^{-41}m^6s^{-1}$
η	Internal quantum efficiency	0.86
β	Spontaneous emission factor	5×10^{-3}
ρ_{cc}	Cavity-cavity reflection coefficient	0.32
ρ_{ca}	Cavity-air transmission coefficient	0.68
ρ_{ac}	Air-cavity transmission coefficient	0
ρ_{aa}	Air-air reflection coefficient	0
γ	Linewidth of QW-SOA	$2\times10^{13}rad/s$
α_0	Transmission efficient	0.9976
Γ	Confinement factor	0.025
N_0	Transparent carrier density	$1.2\times10^{24}m^{-3}$
W	laser width	$1\mu m$

D	laser thickness	$24.5nm$
L	Laser length	$340\mu m$

Variations of the output power versus the pump current for the above quantum well laser is shown in Fig. 5 which indicates the laser threshold current is $47mA$. The corresponding laser threshold current density is $13.82kA/cm^2$.

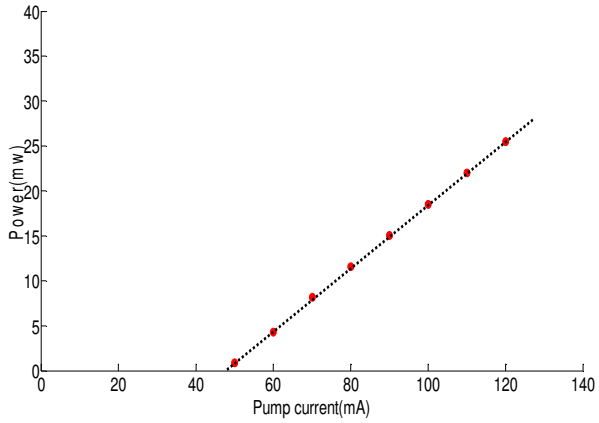

Fig. 5 Power-current characteristics of a $340\mu m$ long quantum well lasers

A. Effects of carrier transport

Figure 6 shows the simulation results of turning-on transients (ToT) of the strained QW laser both with (green) and without (blue) the carrier transport effect (CTE). In our simulation we have assumed the initial ($t=0$) pump current is $50mA$. (the current density is $14.71kA/cm^2$). As the figure shows, the turning-on response can be divided into four stages hereby referred to as $T1$, $T2$, $T3$ and $T4$ where $T1$ is the time period during which the output power varies from zero to the first peak, $T2$ is the time interval between the first peak and the first valley, $T3$ is the stage during which the output power arrives at the second peak from the first valley and $T4$ is the time interval from the second peak to the end. Tab. 2 compares these four time intervals both in the presence and absence of the carrier transport effect.

Table 2 Four stages in the turning-on transient with and without carrier transport effect

Items	$T1$ (ps)	$T2$ (ps)	$T3$ (ps)	$T4$ (ps)
ToT without CTE	0 ~ 32.67	32.67 ~ 57.51	57.51 ~ 98.46	98.46 ~ 290
ToT with CTE	0 ~ 37.92	37.92 ~ 56.62	56.62 ~ 99.36	99.36 ~ 290

Tab. 2 shows that the time intervals $T1$ and $T3$ of the turning-on transient with the carrier transport effect are larger than those without the carrier transport effect. This is because the carriers transporting across the SCH region without being captured by the well region will not take part in the stimulated process, which delays the response speed of the output power. In the stage $T2$, the output power suffers from the gain saturation and decreases. The magnitudes of the first peak ($2mW$) and the second peak ($1.292mW$) without the carrier transport effect are higher than those ($0.857mW$ and $0.735mW$) with the carrier transport effect. Also, carrier transport causes the decreased steady output power in the turning-on transients, which is due to lower average carrier density level in the well.

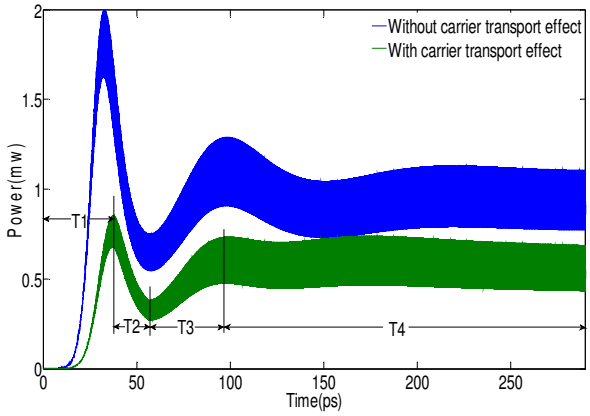

Fig. 6 Turning-on transients of strained QW lasers without (blue) and with (green) carrier transport effect

Figure 7 shows the output power spectral densities with and without carrier transport effect at the steady stage (after $250ps$). The peak magnitudes of the output power spectral densities with and without the carrier transport effect are $-22.72dBm$ and $-16.35dBm$, respectively. Carrier transport has induced a red shift in the laser output spectra; the central frequency of the output power spectral densities has shifted from $195.318THz$ to $195.315THz$ (the difference is $2.563GHz$). Also, Carrier transport decreases the bandwidth of the laser output spectra from $180.78THz$ to $178.75THz$. This is because CTE reduces the carrier density level in the well region which lead to the red shift and bandwidth narrowing of the gain spectrum.

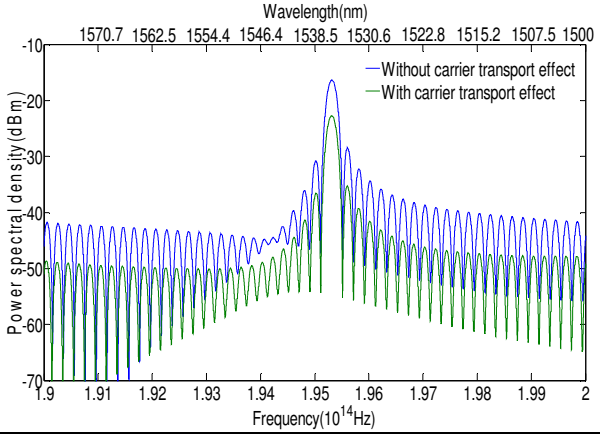

Fig. 7 Output power spectral density at the steady state with (green) and without (blue) carrier transport effect

Figure 8 compares the output power spectral densities during the initial oscillation process (i.e. at the first peak where $t = 37.9\,ps$) and that of steady state (i.e. for $t > 100\,ps$). Comparison of the two output spectra reveals that during the oscillation process both the central frequency and 3-dB bandwidth are higher. In the initial oscillation process, the central frequency and the bandwidth of the power spectral density (blue curve in Fig. 7) are $195.317THz$ and $183.34THz$, respectively. Also, at $t = 37.9\,ps$ the peak magnitude of the output power spectral density is $-19.43dBm$.

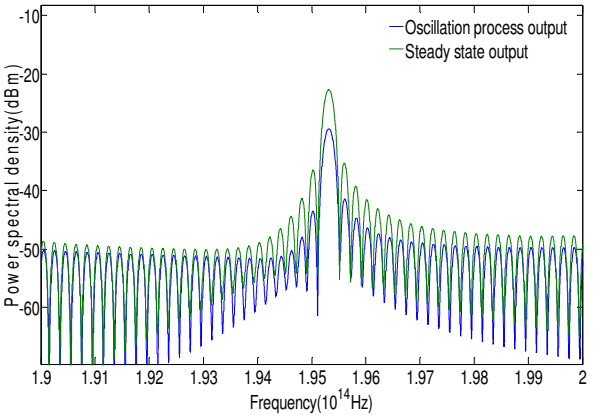

Fig. 8 Output power spectral density with the carrier transport effect at the oscillation process (around $37.9\,ps$) and the steady state

The effects of carrier transport on the turn-off transients of QW lasers are shown in Fig. 9. At $t = 0$, the input current of QW laser is set to be zero. The times taken for the output power to decrease to 0.2mW are 33.47ps with the carrier transport effect included and 2.15ps without considering the carrier transport effect. Carrier transport induces an apparent turn-off delay due to the large transport time across the SCH region.

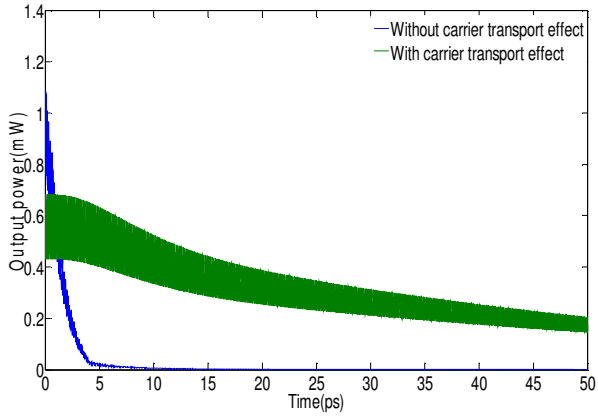

Fig. 9 Turning-off transients of QW lasers (a) with carrier transport effects (b) without carrier transport effects

Figure 10 compares the simulation results of turning-on transients of strained QW lasers obtained by the QW-TLM laser model and the conventional rate equation laser model [24]. It was found that although there exists slight difference in the arriving times of the first peak and the first valley of the turning-on transients ($\Delta T1 = 2.7\,ps$ and $\Delta T2 = 3.7\,ps$), the curves of the turning-on transients analyzed by the two models exhibits the consistent variation trend. The turning-on transient curve obtained by the QW-TLM laser model has a larger line width (as ΔL labelled in Fig. 10), which is because the QW-TLM laser model has considered the scattering relaxing process during the electron transitions. Besides, the QW-TLM laser model can provide the corresponding laser output spectrum at any time as analyzed in the above sections, which is difficult to be realized by the conventional rate equation laser model. This is because the rate equation of photon densities can only describe the optical signal propagation for a longitudinal mode.

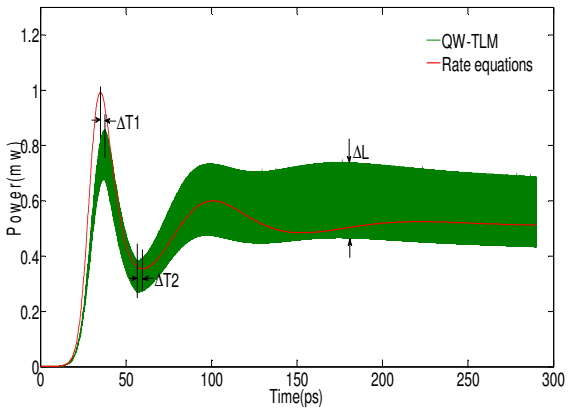

Fig. 10 Turning-on transients of strained QW lasers based on the QW-TLM laser model and conventional rate equations model

B. Effects of pump current spike

In the following, we used the above QW-TLM laser model to make the small signal analysis of pump current spike effects on

the laser output spectra. A pump current spike is applied to the laser after the output has reached the steady state. The current spike is represented by an impulse with a peak value $100mA$ and the width $0.5ps$ as shown in Fig. 11.

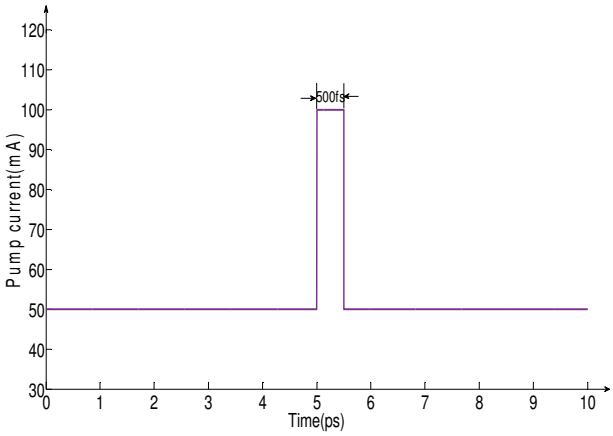

Fig. 11 pump current spike

Figure 12 shows the effects of pump current spike on the laser output spectra. Tab. 3 also compares the important parameters of the output spectra with and without the pump current spike (PCS).

Table 3 Output spectral parameters with and without pump current spike

Parameter	Peak value	$3-dB$ bandwidth	Central frequency	SLSR
Without PCS	$-22.72dBm$	$178.75THz$	$195.315THz$	$12.624dB$
With PCS	$-23.44dBm$	$180.54THz$	$195.317THz$	$12.155dB$

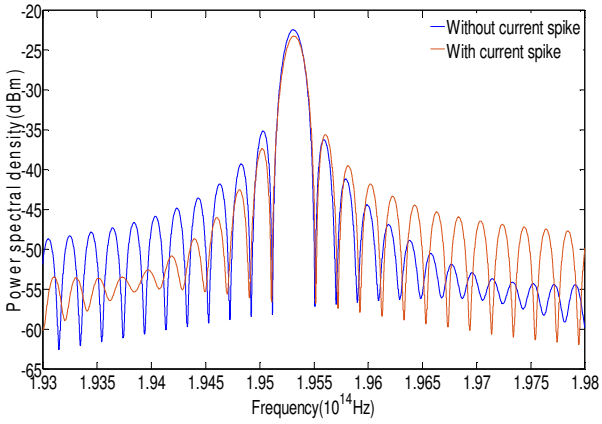

Fig. 12 Effects of current spike on the laser output spectra

Table 3 clearly indicates that the current spike has broadened the laser output spectra bandwidth, induced an apparent red shift in the output spectra and shifted the central frequency from $195.315THz$ to $195.317THz$. The peak values of the output spectra with and without the current spike are $-23.44dBm$ and $-22.72dBm$, respectively, which indicates that although the pump current spike can increase the output power in the time domain, it lowers the peak value in the frequency domain. The side lobe suppression ratios (SLSR) are $12.624dB$ (without PCS) and $12.155dB$ (with PCS). This shows that the pump current spike has reduced the SLSR of the laser output spectrum.

4. CONCLUSIONS

In this paper, a new model for strained QW lasers considering the effects of carrier transport and carrier heating is presented based on the quantum well transmission line modelling method, which can be used to analyze the temporal and spectral properties of QW lasers. The new model is employed to study the effects of carrier transport on the output properties of strained QW lasers and it has been found that in the time domain the carrier transport induces both damping and time delay in the turning-on transients of the laser and in the frequency domain carrier transport causes the red shift, narrowing bandwidth and reduction in the magnitude of the laser output spectra. The simulation results of the turning-on transients obtained by the proposed model are compared with that obtained by the convention rate equation laser model. Also, the effects of pump current spike are studied based on QW-TLM laser model and it was found that a current spike induces the red shift, enhances the bandwidth, reduces the magnitude of the laser output spectrum and decreases SLSR. The new proposed QW laser model is able to accurately study the temporal and spectral behaviors of QW lasers.

REFERENCES

1. C. Gmachl, D. L. Sivco, R. Colombelli, F. Capasso, and A. Y. Cho, "Ultra-broadband semiconductor laser," Nature **415**, 883–887 (2002).

2. Huolei Wang, Hongyan Yu, Xuliang Zhou,Q. Kan Lijun Yuan, Weixi Chen, Wei Wang,Ying Ding and Jiaoqing Pan, "High-power InGaAs/GaAs quantum-well laser with enhanced broad spectrum of stimulated emission," Appl. Phys. Lett. **105**, pp. 141101 1-4 (2014).

3. P. Ludewig, N. Knaub, N. Hossain, S. Reinhard, L. Nattermann, I. P. Marko, S. R. Jin, K. Hild, S. Chatterjee, W. Stolz, S. J. Sweeney and K. Volz, "Electrical injection Ga(AsBi)/(AlGa)As single quantum well laser," Appl. Phys. Lett. **102**, 242115 1-3 (2013).

[3] N. Tessler and G. Eisenstein, "Transient carrier dynamics and photon assisted transport in multiple-quantum-well lasers," IEEE Photon. Tech. Lett., **5**, 291-293 (1993).

[4] H. Hirayama, J. Yoshida, Y. Miyake, and M. Asada, "Carrier capture times and its effect on the efficiency of quantum-well lasers," IEEE J. Quantum Electron., **40**, 5441 (1994).

[5] S. Bennett and C. M. Snowden, "Nonlinear dynamics in directly modulated multiple-quantum-well laser diodes", IEEE J. Quantum Electron., **33**, 2076-2083 (1997).

[6] A. J. Lowery, "A new dynamic multimode model for external cavity semiconductor lasers," IEE Proc. J., **136**, 229-237 (1989).

[7] W. M. Wong and H. Ghafouri-Shiraz, "Dynamic model of tapered semiconductor lasers and amplifiers based on transmission line laser modeling," IEEE Jour. Select. Top. Quant. Elec., **6**, 585-593 (2000).

[8] L. V. T. Nguyen, A. J. Lowery, P. C. R. Gurney, and D. Novak, "A time-domain model for high-speed quantum-well lasers including carrier transport effects," IEEE J. Select. Topics Quantum Electron., **1**, 494–504 (1995).

[9]A.J. Lowery, "Transmission-line modelling of semiconductor lasers: the transmission-line laser model," International Journal of Numerical Modelling, **2**, 249-265 (1989).

[10] A.J. Lowery, "Efficient material-gain models for the transmission-line laser model," International Journal of Numerical Modelling., **2**, 249-265 (1989).

[11] M Xia and H. Ghafouri-Shiraz, "A new optical gain model for quantum wells based on quantum well transmission line modelling method," IEEE J. Quantum Electron., **51**, 2500108, (2015).

[12] H. Ghafouri-Shiraz, "The theory of semiconductor laser diodes and amplifiers: analysis and transmission line laser modelling", Imperial College Press, Singapore, 2004

[13]R. Nagarajan, T. Fukushima, M. Ishikawa, J. E. Bowers, R. S. Geels, and L. A. Coldren, "Transport limits in high-speed quantum-well lasers: Experiment and theory," IEEE Photon. Technol. Lett., **4**, 121-123 (1992).

[14] A. Grabmaier, M. Schofthaler, A. Hangleiter, C. Kazmierski, M. Blez, A. Ougazzaden, "Carrier transport limited bandwidth of 1.55 pm quantum-well lasers," Appl. Phys. Lett., **62**, 52-54 (1993).

[15] Willatzen, M. , Takahashi, T. ,Arakawa, Y. "Nonlinear gain effects due to carrier heating and spectral holeburning in strained-quantum-well lasers" IEEE Photon. Technol. Lett., **4**, 682-685 (1992).

[16] T. Fukushima, A. Kasukawa, M. Iwase, T. Namegaya, and M.Shibata, "Small turn-on delay time in 1.3 pm InAsPlInP strained double quantum-well lasers with very-low threshold current," IEEE Photon. Technol. Lett., **5**, 117-119 (1993).

[17] B. N. Gomatam and A. P. DeFonzo, "Theory of hot carriers effects on nonlinear gain in GaAs/GaAlAs lasers and amplifiers," IEEE J. Quantum Electron., **26**, 1689–1704 (1990).

[18] E. P. O'Reilly and A. R. Adams, "Band-structure engineering in strained semiconductor lasers," IEEE. Quantum Electron., **30**, 366–379, (1994).

[19] C. Y -P. Chao and S L Chuang, "Spin-orbit-coupling effects on the valence-hand structure of strained semiconductor quantum wells," Phys Rev E, **46**, 411M122 (1992).

[20] C. Chang and S. Chuang, "Modeling of strained quantum-well lasers with spin-orbit coupling," IEEE J. Sel. Topics Quantum Electron., **1**, 218–229 (1995).

[21] S. L. Chuang, Physics of Optoelectronic Devices. New York: Wiley, 1995.

[22]M. Xia and H. Ghafouri-Shiraz, "Wavelength-dependent femtosecond pulse amplification in wide band tapered-waveguide quantum well semiconductor optical amplifiers," Applied Optics, **54**,10524-10531(2015).

[23] LOWERY, A.J.: 'New inline wideband dynamic semiconductor laser amplifier model', IEE Proc. Pt. J. **135**, 242-250 (1988).

[24] R. Nagarajan, M. Ishikawa, T. Fukushima, R. S. Geels, and J. E. Bowers, "High speed quantum-well lasers and carrier transport effects," IEEE J. Quantum Electron., **28**, 1990-2008 (1992).

[25] J.M. Dailey and T.L. Koch, "Impact of carrier heating on SOA transmission dynamics for wavelength conversion," IEEE Photon. Technol. Lett., 19, 1078–1080 (2007).

[26] M. Xia and H. Ghafouri-Shiraz, "Analysis of carrier heating effects in Quantum Well semiconductor optical amplifiers considering holes' non-parabolic density of states," Optical Quantum Electronics, 47. 1847-1858 (2015).